

ANN Based Control of Nineteen Level Modular Voltage Source Converter for Single Stage PV – Grid Integration

S Ravi Teja *[‡], Kishore Yadlapati **

* Department of Electrical and Electronics Engineering, Research Scholar, JNTU Kakinada

** Department of Electrical and Electronics Engineering, Assistant Professor, University College of Engineering Narasaraopet, JNTU Kakinada

(srungaramraviteja@gmail.com, kyadlapati@ieeee.org)

[‡] Corresponding Author; Research Scholar, JNTU Kakinada, Kakinada 533003, Andhra Pradesh, India,

Tel: +91 850 091 6362, srungaramraviteja@gmail.com

Received: 18.09.2022 Accepted: 02.11.2022

Abstract- This paper presents ANN based control of nineteen-level modular inverter for single stage PV integration to grid. The inverter operation, filter design and integrated control of single stage power conversion are presented. The control objectives are maximum power extraction and unity power factor current injection to grid. The simulation study of the topology and control is carried out in MATLAB/SIMULINK and an experimental setup for 2.5 kW is developed. Effectiveness of the designed filter is verified in terms of load current harmonic profile. The economic advantage of the topology is validated through comparison in terms of inverter and filter component sizing with similar switch count neutral point clamped inverter. The effectiveness of the control algorithm is validated for steady and transient conditions.

Keywords Grid filter; modular inverter; PV-grid integration; multi-level inverter, ANN.

1. Introduction

The topology of power conversion stage, interfacing filter and control structure of power electronic interface plays a crucial role in the overall performance of multi-MW capacity medium voltage grid connected photo-voltaic (PV) systems with respect to size, cost, efficiency, adaptability, and reliability. The selection of topology depends on quantity of power harness, placement of PV arrays and economic considerations. Centralized non-isolated dc-dc converter and two-level voltage source inverter is the former power electronic interface with the demerits of low efficiency, large filter requirement and reliability. Therefore, there is growing interest towards the application of modular converters in the interfacing topologies owing to independent control and reliability. Multiple grid connection point topologies are most common in low voltage integration system [1] to improve the reliability. A review on the requirements to integrate renewable sources to grid was presented [2] which summarize the standards, sizing, and control aspects. A comparison of centralized arrangement to distributed modular arrangement is reported [3], which appreciate the performance of later in terms of annual energy yield, efficiency and leveled cost of energy. A centralized modular multi-level inverter in dc-ac stage with modular converters in dc-dc boost stage is developed [4], which avoided the problems of reactive power transmission and

harmonic resonance. Multiple dual active bridge converters to achieve isolated dc busses which are then converted to line frequency ac voltage through H-bridge inverter and finally cascaded to achieve required voltage level from low voltage common dc bus of multiple photovoltaic arrays [5]. Input independent and output series connected modular dc-dc converters with inter-module power balancing units is proposed [6]. Modular multi-level converter with independent PV arrays as sources of dc-dc stage for wave shaping followed by dc-ac stage is developed [7]. The advancement in digital control strategies such as hybrid SPWM techniques, neutral shift with power feed-forward control, parallel connected modules control, control scheme for resonant operation of modular converter with inherent voltage balancing capability [8], soft switching control in dc-dc stage [9], common mode voltage minimization [10] has made above modular converters feasible to PV-Grid integration application with improved reliability, redundancy and independent control, however at the cost of increased control complexity, component count and de-rating of the power electronic components owing to sub-module structures. On the other hand, various unconventional topologies were developed to obtain multi-level ac voltage and with appropriate control strategies, minimized interfacing filter size and component count. Nine different generalized topologies were presented [12] in which level generation is carried out in first stage and polarity generation

in second stage. Symmetric and asymmetric staircase cascading multi-level inverter topologies were presented [13]. in which the performance is evaluated in terms of power distribution factor among the modules, blocking voltage, number of switches and switching losses compared to conventional topologies. Switching capacitor topologies also found good performance for dc-ac conversion [14]. However, these unconventional topologies require specially synthesized control structures and are prone to reliability considerations. Therefore, the present work attempts to combine the reliability and redundancy merits of modularity with reduced component count, efficient and stringent design of voltage source inverter topology. The essence of the filter design algorithms stated in [15] is adopted for the proposed topology in the present work. Various control algorithms were developed to integrate the PV power for multi-level inverters like unbalanced grid handling [16], proportional multi resonant control [17], distributed MPP control for multi-string integration [18] and current control of single stage conversion with PV arrays directly feeding the inverter stage [19]. Implementation of low power electronic current controller was reported [20]. Utilization of heuristic and artificial intelligent techniques for power control in renewable energy systems integrated to grid was reported [21]-[29] in which atom search optimization, fuzzy logic-based control, predictive control was adopted for efficient and robust control. The coordination and synchronizing issues under various faults were discussed [30]- [32] in which multiple constraints were considered in integrating hybrid renewable systems to grid. Power quality issues during renewable integration were dealt [33]-[34] This paper presents filter design and artificial neural network (ANN) based current control aspects for a non-conventional, yet modular topology for PV power integration to grid by combining the advantages of reliability, component reduction and single stage power conversion.

The rest of the paper is organized as follows. Section 2 presents the nineteen-level inverter-based topology for high power PV integration to grid. Design of grid side low pass filter is presented in Section 3. Section 4 presents simulation results and performance validation of the system. Section 5 presents the conclusion of the paper.

2. Nineteen Level Modular Inverter-based Interface

The schematic of nineteen-level modular inverter-based PV-grid integration topology is depicted in Fig.1. The PV arrays in each phase directly feed the nineteen-level modular inverter. A low pass filter followed by interfacing transformer at the output of inverter feed the power to the medium voltage grid. Fig.2 depicts three-phase schematic, in which the total available PV power source is grouped into nine arrays with three arrays per phase, such that the dc voltages of A1, A2 and A3 for phase 'a' would be in the ratio of 6:2:1, which feed the inverter through respective dc link capacitances. The similar structure is followed for phase 'b'

and phase 'c'. The transformer model is also included in the three-phase source as shown and M1 and M2 represent the modules of inverter also presented

2.1. Grid Side Low Pass Filter Design

An economic filter design is resorted in this paper. The choice of selecting LCL low pass filter pertains to its higher admittance roll-off beyond resonant frequency. The topology of grid side low pass filter is given in Fig.3. V_1 , i_1 are inverter side ac voltage and current. V_2 , i_2 are grid voltage and injected current into grid. The figure also depicts grid side and inverter side inductor and filter capacitor all with parasitic elements, although which are not considered in design process. Also, the major portion of grid side inductance is determined from the leakage impedance of interfacing transformer. The filter design depends on topology and control structure of the inverter. However, the procedure stated in [15] is followed, where in making the necessary modifications according to the considered topology and control structure.

The focused transfer functions for filter design include inverter current to inverter voltage (self-admittance, Y_{11}) and grid current to inverter voltage (forward admittance, Y_{21}). The frequency response (magnitude) of admittances is shown in Fig.4. This explains the better elimination of frequency components in grid current beyond 1.5 decade of resonant pole. The resonant frequency shall be such that it cannot be much lower than switching frequency or too high for control bandwidth. Sufficient attenuation by reducing forward admittance and minimized effect on control is to be observed. To reduce the forward admittance, one may increase L_1 or L_2 or decrease resonant frequency. As L_1 is expensive element and L_2 is to be realized through leakage impedance of interfacing transformer. Selection of normalized resonant frequency by the inspection of worst-case harmonic spectrum would provide reasonable attenuation to all higher order harmonics. The design of inverter side inductor (L_1) is highly significant for overall size of the system. The selection of low order resonant frequency as explained in previous section makes the shunt impedance to be treated as short circuit at significant harmonics, at the order of switching frequency where L_1 alone is responsible for the rate of rise of inverter current. As it must deal with these higher frequencies, it is more expensive element. so is to be minimized. The maximum ripple in the current is utilized to estimate the optimal value of L_1 as explained here. The worst-case ripple in current is possible in the highest slope of inverter ac voltage applied to filter, which is at zero crossing regions. L_2 and C_3 from will be chosen to minimize filter size and thus cost. Leakage impedance form minimum inductance requirement for L_2 and the rounding value of L_2 is to be determined from the fact that, for maximum power to be transferred for given constant grid voltage, higher the maximum voltage of inverter so would be L_2 . C_3 is selected for stiff DC bus.

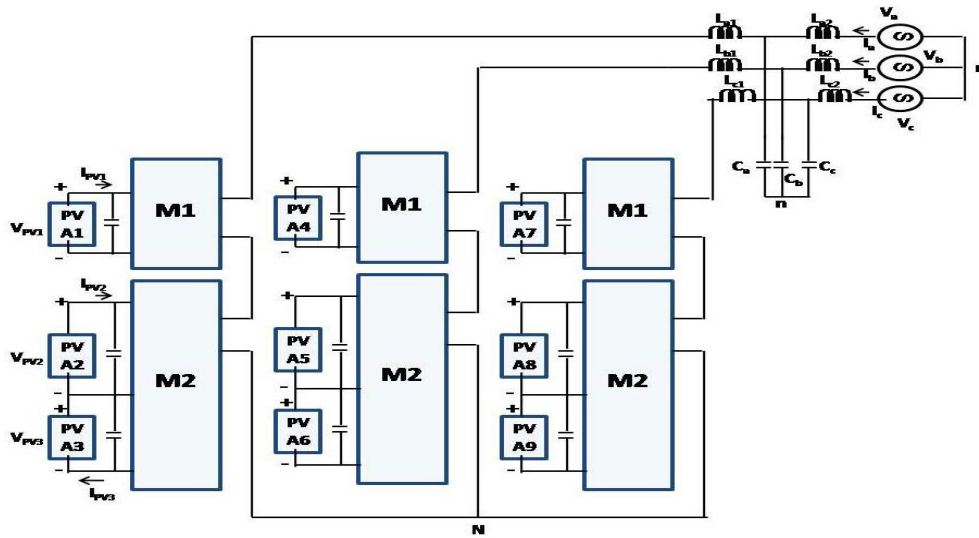


Fig. 1. Nineteen-Level Modular Inverter based PV-Grid integration

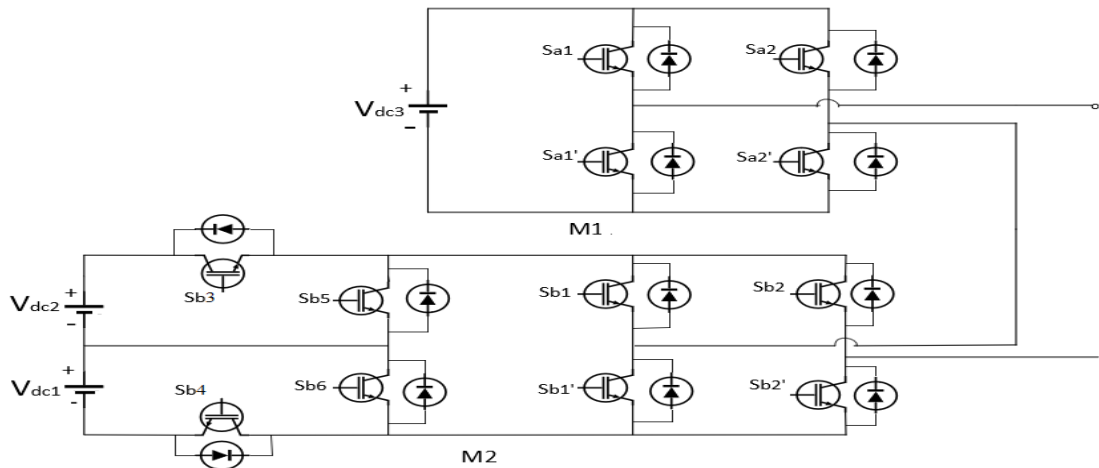


Fig. 2. Nineteen-level modular inverter topology

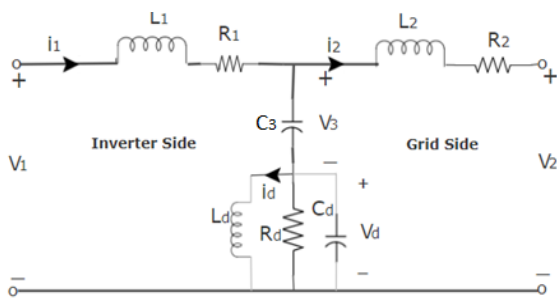


Fig. 3. Grid side low pass filter

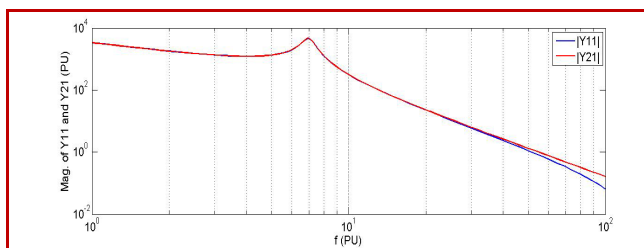


Fig. 4. Admittance magnitude vs normalized frequency

3. ANN Based Control of Power Conversion

Control structure of the voltage source inverter for integration of PV power to grid is shown in Fig.5. The topology and control eliminate the need of dc-dc converters. Maximum power absorption is integral part of voltage source inverter control with maximum range of modulation index, being in the control range of PI controller for all possible irradiation patterns. The objectives of the power flow control are maximum power extraction from PV source and power injection into grid at unity power factor. Voltages and currents of individual arrays feed maximum power point tracking (MPPT) block, which determine reference DC voltages of inverter. The proportional plus integral (PI) controller with combined errors in dc bus voltages as input, determines the magnitude of current. Unit templates of grid phase voltages multiplied by reference current magnitude generate the reference current of respective phases. The error in actual and reference phase currents serve as input to pulse generator with nine-level m-carrier as shown in Fig.6.

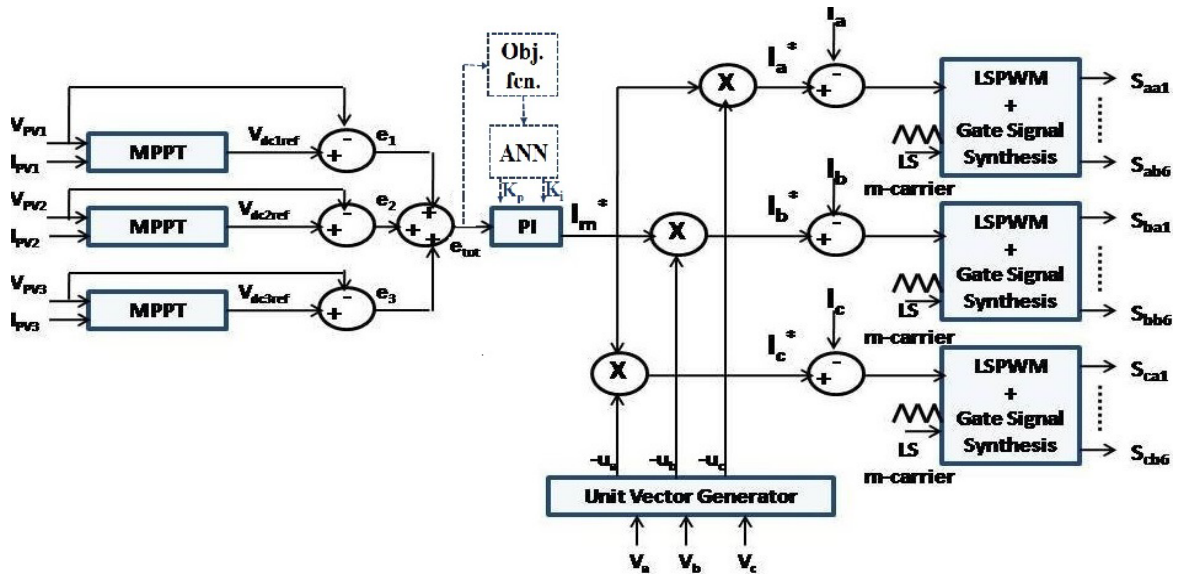


Fig. 5. ANN based control algorithm for power conversion

The pulse width modulation (PWM) patterns obtained by comparison of reference signal with positive level carriers and that with negative level carriers are designated are logically added (OR operation) to generate gating pulses for the combination of switches in each level.

4. Simulation and Experimental Results

Simulation of PV power integration the topology with proposed control algorithm is carried out in MATLAB/SIMULINK and experimentation with 2.5 kW PV source is carried out. The experimental setup is shown in Fig. 7. The system parameters are provided in Table 1. The effectiveness of filter design and control are presented in this section.

4.1. Effectiveness of Grid side Low Pass Filter Design

The inverter operation is considered under nine conditions, which include operating power factor range (0.9 sinking, UPF, 0.9 sourcing) and voltage modulation index over the range 0.85 to 1.15. The magnitudes of total harmonic distortion (THD) are measured for inverter output line voltage and current. As identified from the Fig.8, the THD in each case is largely above the respective limit.

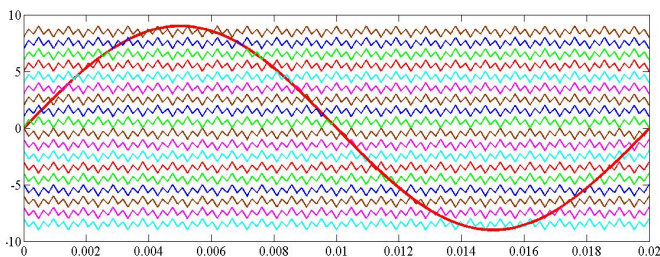


Fig. 6. Reference signal and level shifted modified triangular carrier



Fig. 7. Experimental Setup

Table 1. Simulation and experimental parameters

| Parameter | Simulation | Experimentation |
|--|-------------------|-------------------|
| PV Power Rating | 1 MW | 2.5 kW |
| $V_{PV1}, V_{PV2}, V_{PV3}$ (for each phase) | 40 V, 80 V, 240 V | 40 V, 80 V, 240 V |
| Rated inverter output voltage | 230 V (RMS) | 230 V (RMS) |
| L_1 | 0.18 pu | 0.18 pu |
| L_2 | 0.07 pu | 0.07 pu |
| C_3 | 0.77 pu | 0.77 pu |
| K_p, K_i | 0.25, 0.9 | 0.25, 0.9 |

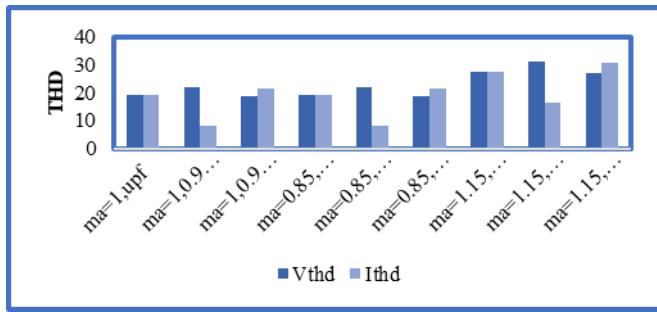
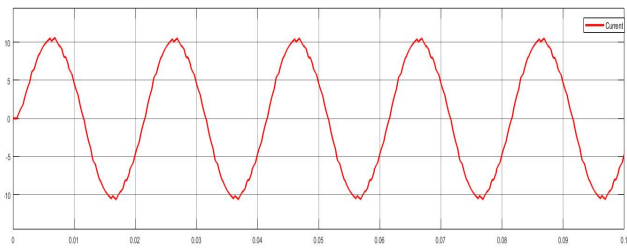
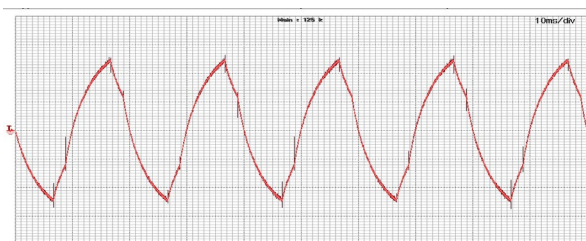


Fig. 8. Worst case contributions of various voltage and current harmonics over system operating range

The filter component values shown in Table 2 are obtained according to the procedure stated in section 2. L1 is estimated for maximum ripple of 0.05 pu. Fig.9 shows the measured RL load current with filter, which validates the design estimation of L1. THD for different loads in operating power factor range is shown in Fig. 10 which validates the THD is under IEEE 519 std. limit in complete operating range. The load current THD in operating modulation index and power factor range with and without filter are shown in Fig.11 and Fig.12 respectively. The economic advantage of the inverter and filter combination is presented in terms of comparison of semi-conductor and copper requirement with respect to similar switch count neutral point clamped (NPC) inverter-based interface is shown in Table 2.



(a)



(b)

Fig. 9. RL Load current with filter (a) Simulated (b) Experimental

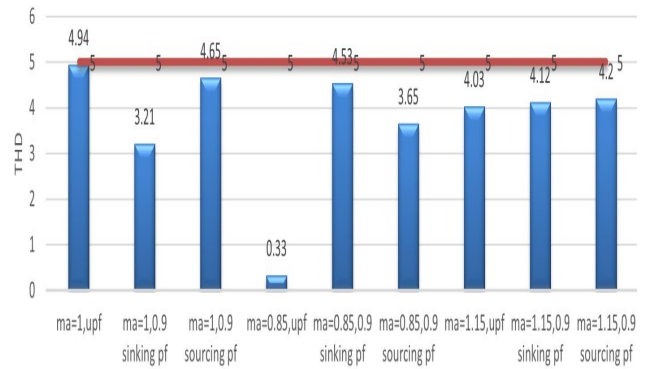


Fig. 10. Load Current THD with filter

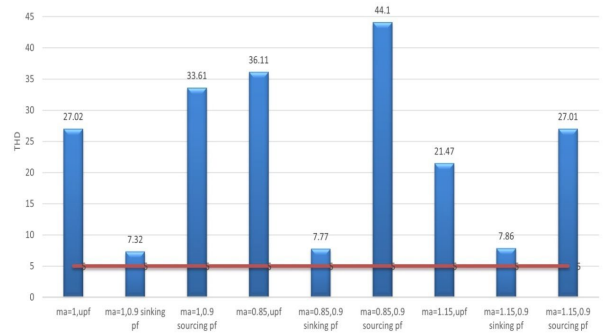


Fig. 11. Load Current THD without filter with seven level NPC inverter

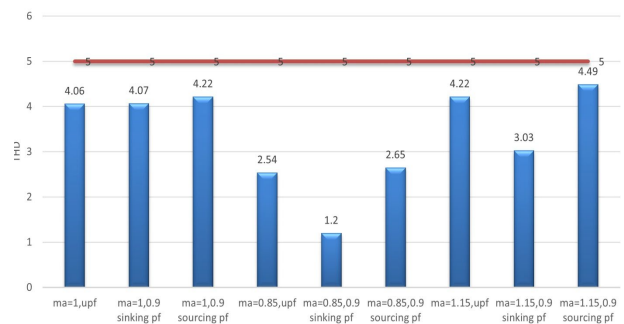


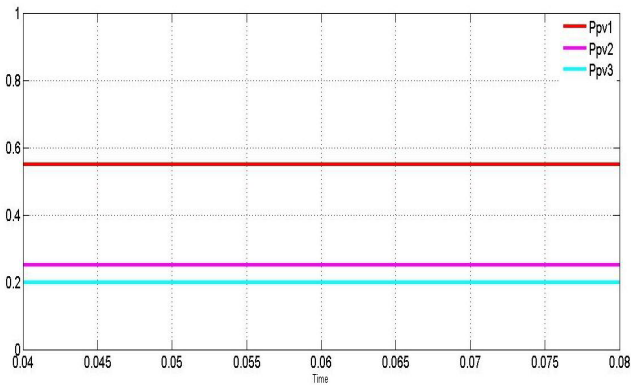
Fig. 12. Load Current THD with filter with seven level NPC inverter

Table 2. Switches and filter sizing Comparison

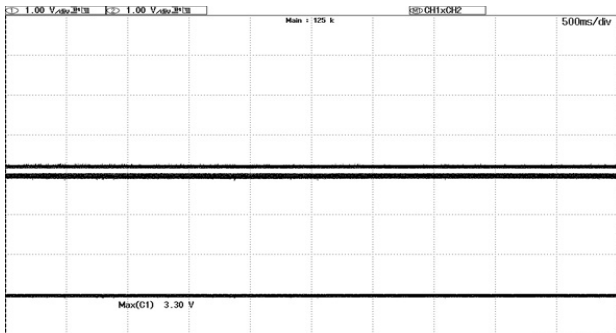
| Topology | V _{swavg} (pu) | I _{swavg} (pu) | L ₁ (pu) | L ₂ (pu) |
|----------------------------------|-------------------------|-------------------------|---------------------|---------------------|
| Nineteen- level modular inverter | 0.44 | 0.43 | 0.18 | 0.07 |
| Neutral point clamped inverter | 0.5 | 1 | 0.313 | 0.1 |
| Percentage economic advantage | 12 | 57 | 42.4 | 30 |

4.2. Maximum Power Extraction

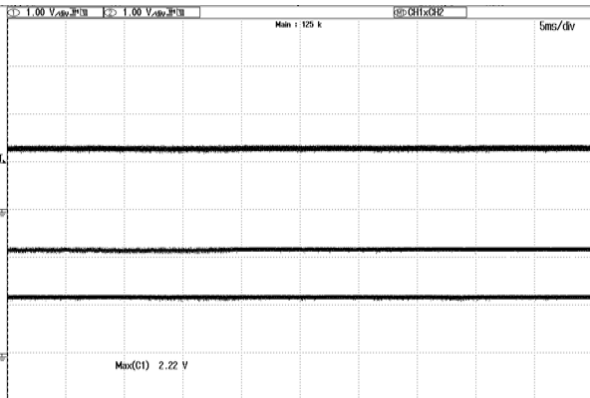
The MPP algorithm, which determines the required dc bus voltage for each array has the additional advantage of reducing the burden of PI controller providing sufficient tracking time to trace the slowly varying dc bus voltages. The steady maximum power and steady dc voltages from each array at 1000 W/m² is shown in Fig.13 and Fig. 14 respectively. Also, the tracking of new maximum power point for a step change in irradiance from 600 W/m² to 800 W/m² is shown in Fig.15. The performance of integrated MPP control can be observed form quick tracking of new maximum power point for change in irradiance.



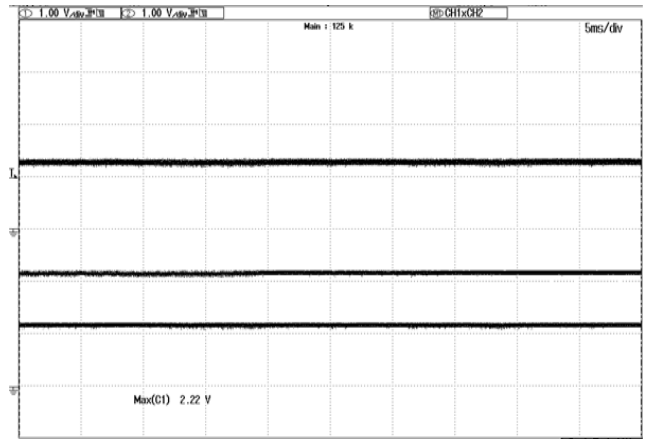
(a)



(b)

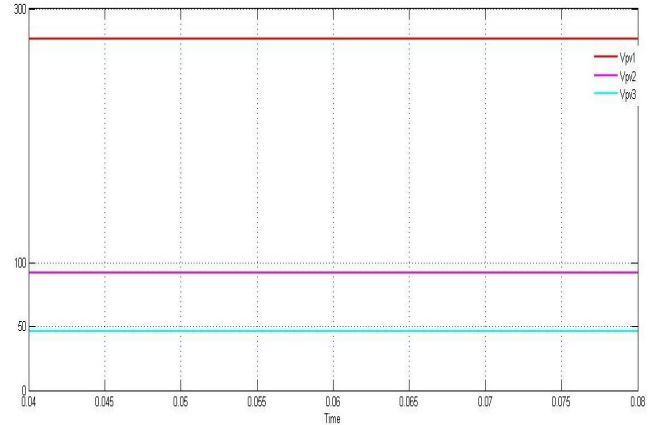


(c)

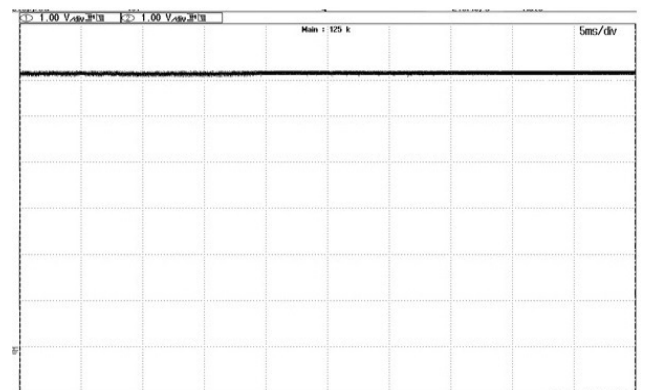


(d)

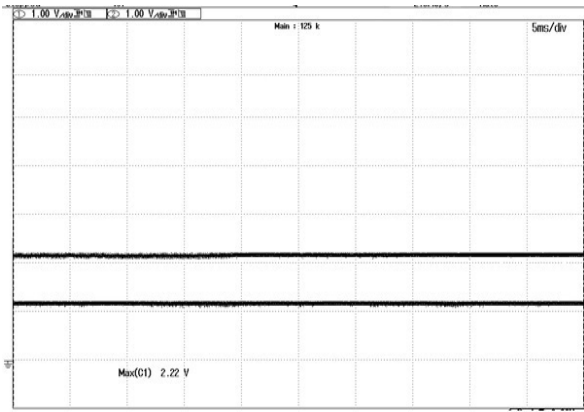
Fig. 13. (a) Simulation result for Maximum power for three PV arrays at 1000 W/m² irradiance (b) Experimental Voltage, Current and Power for PV A1 (c) Experimental Voltage, Current and Power for PV A2 (d) Experimental Voltage, Current and Power for PV A3



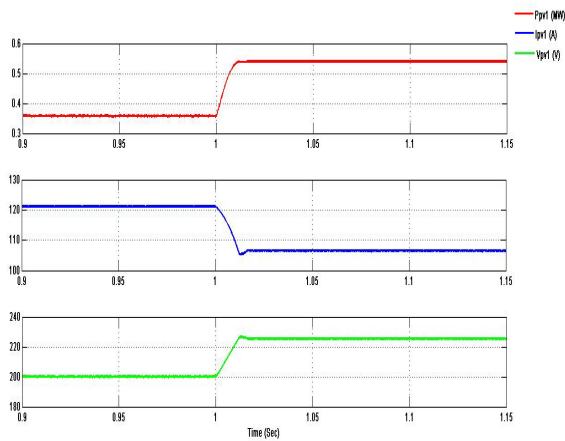
(a)



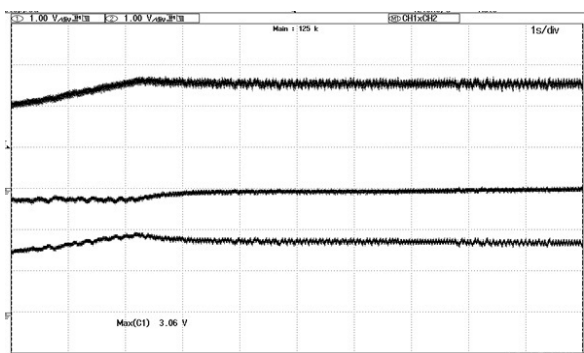
(b)



(c)
Fig. 14. Output voltages of PV arrays (a) Simulation (b) Experimental waveform for PV A1 output voltage (c) Experimental waveforms for PV A2 and PV A3 output voltage



(a)



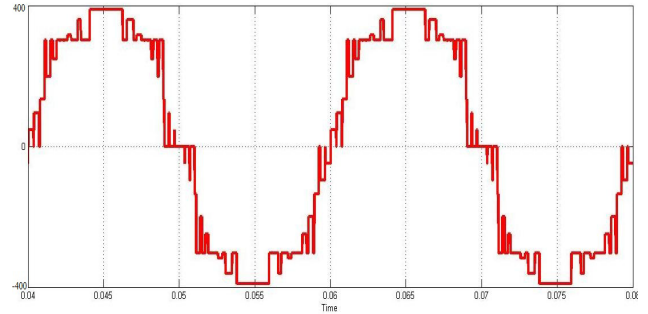
(b)

Fig. 15. Maximum power point tracking for change in irradiance for PV A1 (a) Simulated (b) Experimental

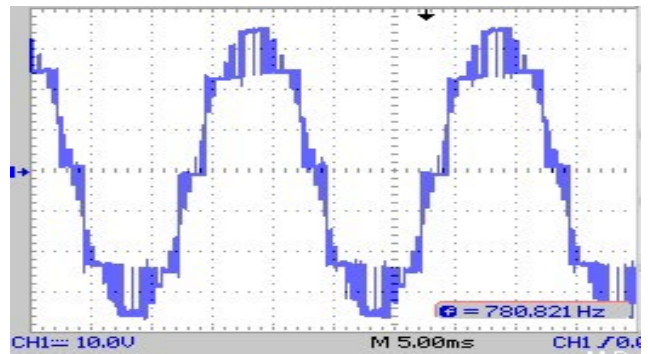
4.3. Unity Power Factor Power Export

This single stage power integration does not regulate the dc bus. Instead, the control provides the modulation of inverter output voltage such as to absorb maximum power

from the PV arrays and pump into the grid. The Fig.16 and Fig. 17 respectively present the effective modulation of inverter output voltage and power injection to grid at unity power factor current. The employed current control, thus present the precise tracking of the reference current.

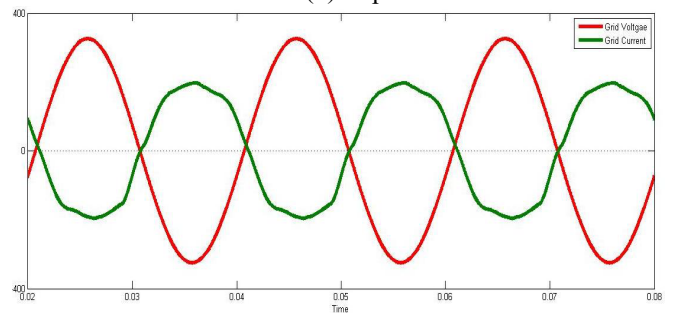


(a)

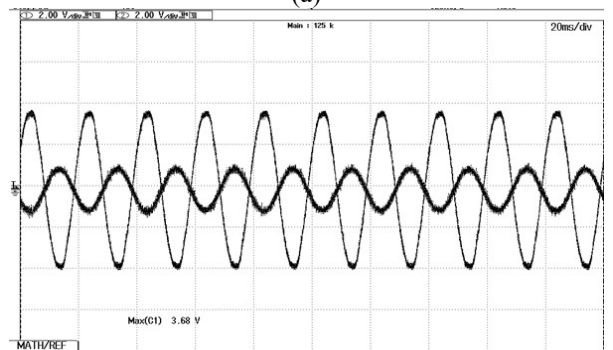


(b)

Fig. 16. Inverter output voltage for 1000 W/m² irradiance (a) Simulated (b) Experimental



(a)



(b)

Fig. 17. Unity power factor current injection into grid
(a) Simulation (b) Experimental

5. Conclusions

A novel topology for PV-Grid Integration is presented with modular single stage conversion which achieved modularity with low component count. A nineteen-level output voltage was achieved with 12 switches per each leg where only seven level output voltage was achievable with similar count conventional topologies. Grid side filter is designed based on worst case harmonic spectrum which resulted in 30 percent saving in size with respect to seven level NPC based interface. The effectiveness of the filter design is validated in terms of load current harmonic profile which is less than 5 percent for all load conditions. Also, the individual harmonic components were also under compliance for grid integration. A 12 percent reduction in voltage sizing and 57 percent in current sizing was achieved for the converter switches which validate the economic benefit of the proposed topology. The control algorithm was proved robust for maximum power tracking and unity power factor power export to grid. Coordination among the three phases was the primary challenges in this topology. Improving the control strategy to solve unbalance issues would be future scope for the work.

References

- [1] J C. D. Fuentes, C. A. Rojas, H. Renaudineau, S. Kouro, M. A. Perez and T. Meynard, "Experimental Validation of a Single DC Bus Cascaded H-Bridge Multilevel Inverter for Multistring Photovoltaic Systems," in *IEEE Transactions on Industrial Electronics*, vol. 64, no. 2, pp. 930-934, Feb. 2017, doi: 10.1109/TIE.2016.2619661.
- [2] Korhan Kayisli, Ruhi Zafer Caglayan, Nurkhat Zhakiyev, Abdulkader Harrouz, Ilhami Colak, "A Review of Hybrid Renewable Energy Systems and MPPT Methods," in *International Journal of Smart Grid*, vol. 6, no. 3, Sep. 2022.
- [3] A. B. Acharya, M. Ricco, D. Sera, R. Teodorescu and L. E. Norum, "Performance Analysis of Medium-Voltage Grid Integration of PV Plant Using Modular Multilevel Converter," in *IEEE Transactions on Energy Conversion*, vol. 34, no. 4, pp. 1731-1740, Dec. 2019, doi: 10.1109/TEC.2019.2930819.
- [4] Wu, P., Huang, W. and Tai, N. (2019), Novel grid connection interface for utility-scale PV power plants based on MMC. *The Journal of Engineering*, 2019: 2683-2686. <https://doi.org/10.1049/joe.2018.8911>.
- [5] T. Liu et al., "Design and Implementation of High Efficiency Control Scheme of Dual Active Bridge Based 10 kV/1 MW Solid State Transformer for PV Application," in *IEEE Transactions on Power Electronics*, vol. 34, no. 5, pp. 4223-4238, May 2019, doi: 10.1109/TPEL.2018.2864657.
- [6] X. Li, M. Zhu, M. Su, J. Ma, Y. Li and X. Cai, "Input-Independent and Output-Series Connected Modular DC-DC Converter With Inter module Power Balancing Units for MVdc Integration of Distributed PV," in *IEEE Transactions on Power Electronics*, vol. 35, no. 2, pp. 1622-1636, Feb. 2020, doi: 10.1109/TPEL.2019.2924043.
- [7] T. S. Basu and S. Maiti, "A Hybrid Modular Multilevel Converter for Solar Power Integration," in *IEEE Transactions on Industry Applications*, vol. 55, no. 5, pp. 5166-5177, Sept.-Oct. 2019, doi: 10.1109/TIA.2019.2928245.
- [8] A. M. Mahfuz-Ur-Rahman, M. R. Islam, K. M. Muttaqi and D. Sutanto, "A Magnetic-Linked Multilevel Active Neutral Point Clamped Converter With an Advanced Switching Technique for Grid Integration of Solar Photovoltaic Systems," in *IEEE Transactions on Industry Applications*, vol. 56, no. 2, pp. 1990-2000, March-April 2020, doi: 10.1109/TIA.2020.2965915.
- [9] R. Suryadevara and L. Parsa, "Full-Bridge ZCS-Converter-Based High-Gain Modular DC-DC Converter for PV Integration With Medium-Voltage DC Grids," in *IEEE Transactions on Energy Conversion*, vol. 34, no. 1, pp. 302-312, March 2019, doi: 10.1109/TEC.2018.2878964.
- [10] S. Du, B. Wu and N. Zargari, "Common-Mode Voltage Minimization for Grid-Tied Modular Multilevel Converter," in *IEEE Transactions on Industrial Electronics*, vol. 66, no. 10, pp. 7480-7487, Oct. 2019, doi: 10.1109/TIE.2018.2881939.
- [11] P. R. Bana, K. P. Panda, R. T. Naayagi, P. Siano and G. Panda, "Recently Developed Reduced Switch Multilevel Inverter for Renewable Energy Integration and Drives Application: Topologies, Comprehensive Analysis and Comparative Evaluation," in *IEEE Access*, vol. 7, pp. 54888-54909, 2019, doi: 10.1109/ACCESS.2019.2913447.
- [12] H. Samsami, A. Taheri and R. Samanbakhsh, "New bidirectional multilevel inverter topology with staircase cascading for symmetric and asymmetric structures. *IET Power Electronics*, 10: 1315-1323, 2017.
- [13] A. I. Elsanabary, G. Konstantinou, S. Mekhilef, C. D. Townsend, M. Seyedmahmoudian and A. Stojcevski, "Medium Voltage Large-Scale Grid-Connected Photovoltaic Systems Using Cascaded H-Bridge and Modular Multilevel Converters: A Review," in *IEEE Access*, vol. 8, pp. 223686-223699, 2020, doi: 10.1109/ACCESS.2020.3044882.
- [14] V. Jammala, S. Yellarsi and A. K. Panda, "Development of a New Hybrid Multilevel Inverter Using Modified Carrier SPWM Switching Strategy," in *IEEE Transactions on Power Electronics*, vol. 33, no. 10, pp. 8192-8197, Oct. 2018, doi: 10.1109/TPEL.2018.2801822.
- [15] S. Jayalath and M. Hanif, "Generalized LCL-Filter Design Algorithm for Grid-Connected Voltage-Source Inverter," in *IEEE Transactions on Industrial Electronics*,

- vol. 64, no. 3, pp. 1905-1915, March 2017, doi: 10.1109/TIE.2016.2619660.
- [16] S. Yazdani, M. Ferdowsi, M. Davari and P. Shamsi, "Advanced Current-Limiting and Power-Sharing Control in a PV-Based Grid-Forming Inverter Under Unbalanced Grid Conditions," in *IEEE Journal of Emerging and Selected Topics in Power Electronics*, vol. 8, no. 2, pp. 1084-1096, June 2020, doi: 10.1109/JESTPE.2019.2959006.
- [17] M. K. Mishra and V. N. Lal, "An Advanced Proportional Multiresonant Controller for Enhanced Harmonic Compensation With Power Ripple Mitigation of Grid-Integrated PV Systems Under Distorted Grid Voltage Conditions," in *IEEE Transactions on Industry Applications*, vol. 57, no. 5, pp. 5318-5331, Sept.-Oct. 2021, doi: 10.1109/TIA.2021.3091046.
- [18] S. R. Pendem, S. Mikkili and P. K. Bonthagorla, "PV Distributed-MPP Tracking: Total-Cross-Tied Configuration of String-Integrated-Converters to Extract the Maximum Power Under Various PSCs," in *IEEE Systems Journal*, vol. 14, no. 1, pp. 1046-1057, March 2020, doi: 10.1109/JSYST.2019.291976.
- [19] S. B. Q. Naqvi, S. Kumar and B. Singh, "Weak Grid Integration of a Single-Stage Solar Energy Conversion System With Power Quality Improvement Features Under Varied Operating Conditions," in *IEEE Transactions on Industry Applications*, vol. 57, no. 2, pp. 1303-1313, March-April 2021, doi: 10.1109/TIA.2021.3051114.
- [20] V. Krishna Murali, V Sandeep, "Design and Simulation of Current Sensor based Electronic Load Controller for Small Scale Three Phase Self Excited Induction Generator System", *International Journal of Renewable Energy Research (IJRER)*, 10(4), 1638-1644, December 2020.
- [21] S. J. Gambhire, M. K. Kumar, K. Mallikarjuna, A. N. Venkateswarlu, C. N. S. Kalyan, and B. S. Goud, "Performance Comparison of Various Classical Controllers in LFC of Hydro-Thermal Power System with Time Delays," in *2022 10th International Conference on Smart Grid (icSmartGrid)* (pp. 401-406), IEEE, June 2022.
- [22] C. R. Reddy, B. S. Goud, F. Aymen, G. S. Rao and E. C. Bortoni, "Power quality improvement in HRES grid connected system with FOPID based atom search optimization technique," *Energies*, 14(18), 5812, 2021.
- [23] S. Benhadouga, A. Belkaid, I. Colak, M. Meddad and A. Eddiai, "Experimental Validation of The Sliding Mode Controller to Improve The Efficiency of The MPPT Solar System," *2021 10th International Conference on Renewable Energy Research and Application (ICRERA)*, 2021, pp. 333-337, doi: 10.1109/ICRERA52334.2021.9598584.
- [24] R. Rekha, B. Srikanth Goud, R. Reddy, and B. Nagi Reddy, "PV-Wind-Integrated Hybrid Grid with P&O Optimization Technique" In *Innovations in Electrical and Electronics Engineering*, pp. 587-600, Springer, Singapore, 2020.
- [25] B. S. Goud, R. Reddy, R. R. Udumula, M. Bajaj, B. Abdul Samad, M. Shouran, , and S . Kamel, "PV/WT integrated system using the Gray Wolf Optimization Technique for power quality improvement", *Frontiers in Energy Research*, 10, 2022.
- [26] B. S. Goud, B. L. Rao and C. R. Reddy, "An intelligent technique for optimal power quality reinforcement in a grid-connected HRES system: EVORFA technique," in *International Journal of Numerical Modelling: Electronic Networks, Devices and Fields*, 34(2), e2833, 2021.
- [27] B. S. Goud, and B. L. Rao "Power quality enhancement in grid-connected PV/wind/battery using UPQC: atom search optimization", *Journal of Electrical Engineering & Technology*, 16(2), 821-835, 2021.
- [28] G. S. Rao, B. S. Goud and C. R. Reddy, "Power Quality Improvement using ASO Technique", In *2021 9th International Conference on Smart Grid (icSmartGrid)*, pp. 238-242, IEEE, June 2021.
- [29] R. Barzegarkhoo, S. A. Khan, Y. P. Siwakoti, R. P. Aguilera, S. S. Lee and M. N. H. Khan, "Implementation and Analysis of a Novel Switched-Boost Common-Ground Five-Level Inverter Modulated With Model Predictive Control Strategy," in *IEEE Journal of Emerging and Selected Topics in Power Electronics*, vol. 10, no. 1, pp. 731-744, Feb. 2022, doi: 10.1109/JESTPE.2021.3068406.
- [30] H. Gaied, M. Naou, H. Kraiem, B. S. Goud, A. Flah, M. L. Alghaythi and K. Aboras, "Comparative analysis of MPPT techniques for enhancing a wind energy conversion system," in *Frontiers in Energy Research*, 10, 2022.
- [31] C. R. Reddy, B. S. Goud, B. N. Reddy, M. Pratyusha, C. V. Kumar, and R. Rekha, "Review of islanding detection parameters in smart grids," In *2020 8th International Conference on Smart Grid (icSmartGrid)*, pp. 78-89, IEEE, June 2020.
- [32] B. Srikanth Goud, Ch Rami Reddy, Mohit Bajaj, Ehab E. Elattar, and Salah Kamel, "Power Quality Improvement Using Distributed Power Flow Controller with BWO-Based FOPID Controller," in *Sustainability*, 13, no. 20 ,2021.
- [33] B. Srikanth Goud, B. Loveswara Rao, Aymen Flah, Mohit Bajaj, Naveen Kumar Sharma, and Ch Reddy, "Biogeography-Based Optimization for Power Quality Improvement in HRES System" In *Power Electronics and High Voltage in Smart Grid*, pp. 309-316. Springer, Singapore, 2022.